Golgi-associated GSK3β regulates the sorting process of post-Golgi membrane trafficking

Atsuhiro Adachi[1], Fumi Kano[1,2], Takashi Tsuboi[1], Morihisa Fujita[3], Yusuke Maeda[3] and Masayuki Murata[1,*]

[1]Department of Life Sciences, Graduate School of Arts and Sciences, The University of Tokyo, Komaba 3-8-1, Meguro-ku, Tokyo 153-8902, Japan
[2]PRESTO, Japan Science and Technology Agency, 4-1-8 Honcho Kawaguchi, Saitama 332-0012, Japan
[3]Research Institute for Microbial Diseases, Osaka University, Suita, Osaka 565-0871, Japan
*Author for correspondence (mmurata@bio.c.u-tokyo.ac.jp)

Accepted 14 June 2010
Journal of Cell Science 123, 3215-3225

doi:10.1242/jcs.063941

Summary

Glycogen synthase kinase β (GSK3β) phosphorylates many substrates in mammalian cells, and functions in many physiological processes. We observed that GSK3β knockdown by siRNA perturbed both Golgi morphology in HeLa cells and the anterograde transport of cation-independent mannose 6-phosphate receptor (CI-M6PR) from the *trans*-Golgi network (TGN) to prelysosomal compartments (PLC), diverting it to the exocytic pathway. Moreover, we demonstrate that a portion of GSK3β was localized to the TGN through the Golgi peripheral protein p230 and that this localization regulated CLASP2 phosphorylation. Our results also show that GSK3β knockdown resulted in accumulation of CLASP2 at microtubule plus ends at the cell periphery. Our findings support the hypothesis that GSK3β at the TGN acts as a guide, activates exocytic transport, and redirects CI-M6PR from transport to the PLC into the exocytic pathway by regulating the affinity of CLASPs for microtubules.

Key words: Golgi, CI-M6PR, CLASP2, GSK3β, Vesicular transport

Introduction

In the *trans*-Golgi network (TGN), proteins destined for the plasma membrane (PM), secretory vesicles, and lysosomes are sorted and exit from the Golgi complex. Mannose-6-phosphate receptors (M6PRs) mediate the transport of newly synthesized lysosomal enzymes with an M6P recognition motif from the TGN to lysosomes. For example, the cation-independent mannose-6-phosphate receptor (CI-M6PR) delivers lysosomal enzymes to the prelysosomal compartment (PLC). In the PLC, the receptor and ligand dissociate, which is necessary and sufficient to allow M6PR recycling to the TGN. Although a small percentage of M6PR is targeted to the cell surface to internalize extracellular ligands, ~90% of the total M6PR pool is intracellular and, in most cells, cycles between the TGN and the PLC (Fischer et al., 1980). Formation of CI-M6PR vesicles from the TGN requires intact microtubules and actin networks (Waguri et al., 2003), and disruption of microtubules with nocodazole impairs lysosomal enzyme transport to endocytic compartments (Scheel et al., 1990).

A variety of kinases localize to the Golgi and regulate post-Golgi membrane trafficking (Bossard et al., 2007; Garczarczyk et al., 2009; Salvarezza et al., 2009). Previously, we found that knockdown of glycogen synthase kinase β (GSK3β) in HeLa cells disrupts intracellular trafficking between the Golgi and endosomes and results in a significant increase in β-amyloid secretion (the hallmark of Alzheimer's disease), as shown by high-content screening using kinase inhibitors and a human kinase siRNA library (Adachi et al., 2009). GSK3β, a mammalian isoform of GSK3, is a serine/threonine kinase and functions in many physiological processes, including disease, cell polarity, microtubule dynamics, and the cell cycle (Grimes and Jope, 2001). GSK3β modulates microtubule dynamics through the phosphorylation of many substrates and regulates both plus- and minus-end microtubules. At the minus end, GSK3β localizes to the centrosome and interacts with Bicaudal-D to regulate centrosomally focused microtubules (Fumoto et al., 2006). GSK3β also regulates the stability of microtubule plus ends by phosphorylating plus-end tracking proteins (+TIPs).

Cytoplasmic linker protein (CLIP)-associating protein 2 (CLASP2) is phosphorylated by GSK3β. CLASPs are microtubule-associated proteins that localize to both the Golgi and microtubule cortical sites, and stabilize local microtubules (Lansbergen et al., 2006). Hyperphosphorylation of CLASP2 by GSK3β disrupts the association between microtubules and CLASP2, which disperses into the cytoplasm (Kumar et al., 2009). Recently, a microtubule subset that is nucleated at the Golgi rather than at the well-known centrosomal microtubule organizing center (MTOC) was discovered by Kaverina's group (Efimov et al., 2007). They demonstrated that Golgi-derived microtubules, which are dependent on CLASPs, are crucial for establishing the continuity and correct morphology of the Golgi and for directional post-Golgi membrane trafficking (Miller et al., 2009). In fact, CLASPs are involved in vesicular transport from the Golgi to the PM by attaching distal microtubule ends to the cell cortex via a complex between LL5β [a phosphatidylinositol (3,4,5)-trisphosphate binding protein] and Rab6-interacting protein (ELKS) (Lansbergen et al., 2006). However, it is unclear how GSK3β modulates differentially CLASPs that localize at the Golgi and those that localize at microtubule cortical sites, and how it affects Golgi morphology and post-Golgi trafficking.

In this study, we found that a portion of GSK3β localized to the TGN through the Golgi peripheral protein p230 and affected post-Golgi membrane trafficking. In GSK3β-knockdown cells, the morphological integrity of the Golgi was disrupted and, in parallel, dephosphorylated CLASP2 accumulated at the plus ends of microtubules at the cell periphery. The perturbation of GSK3β–CLASP2-dependent stabilization of microtubules and the

Journal of Cell Science

morphological integrity of the Golgi complex facilitated exocytic transport and diverted CI-M6PR from transport to the PLC into the exocytic pathway. We hypothesize that GSK3β at the TGN acts as a guide for constitutive exocytic carriers by regulating the affinity of CLASPs for microtubules.

Results

GSK3β localizes to the TGN in HeLa cells and is involved in the maintenance of Golgi morphology

To examine the localization of endogenous GSK3β in HeLa cells, we performed immunofluorescence with an anti-GSK3β antibody and antibodies against various organelle markers. GSK3β was detected as a diffuse fluorescent signal throughout the cytoplasm, but also colocalized with p230 (Fig. 1A) and, in part, with GM130 (Fig. 1A), which are markers of the TGN and *cis*-Golgi, respectively. These results agreed with those obtained by Gärtner and co-workers who reported a substantial association of GSK3β with the Golgi in neuronal cells (Gärtner et al., 2006).

To examine whether GSK3β in the TGN is involved in the maintenance of Golgi morphology, we prepared three different siRNA probes and examined changes in Golgi morphology in GSK3β-knockdown cells. Each siRNA probe reduced the level of GSK3β in HeLa cells to 20–30% of that in control cells (supplementary material Fig. S1A). Cells were treated with scramble (control) or GSK3β siRNA for 72 hours, fixed, and immunostained with anti-GSK3β and anti-p230 antibodies (supplementary material Fig. S1B). We confirmed that gene silencing by all three GSK3β siRNAs caused Golgi fragmentation. siRNA #3 gave the best results, therefore we decided to use siRNA #3 for subsequent experiments. In control cells, immunostaining of markers for various Golgi cisterna showed a typical ribbon-like Golgi. In the GSK3β-knockdown cells, staining of p230 and mannosidase II, a marker of the *medial*-Golgi (Fig. 1B), or GM130 and mannosidase II (Fig. 1C) gave a fragmented pattern. The extent of Golgi fragmentation was estimated by morphometric analysis: ~70% of the Golgi in GSK3β-knockdown cells was fragmented (Fig. 1D). In addition, we measured the average diameter of the area in which p230-positive Golgi fragments were dispersed. The average diameter in GSK3β-knockdown cells was approximately twice that in control cells (supplementary material Fig. S1C). The fragmented Golgi was not dispersed throughout the cytoplasm but rather was concentrated around the centrosome (supplementary material Fig. S1D). FRAP (fluorescence recovery after photobleaching) analysis using cells in which GFP-labeled galactosyltransferase (GT–GFP) was expressed in the TGN revealed that the continuity between the Golgi fragments was disrupted in GSK3β-knockdown cells (supplementary material Fig. S2). These results indicate that GSK3β is involved in the maintenance of Golgi morphology.

CI-M6PR is transported from the Golgi by long tubular carriers after GSK3β knockdown

Immunofluorescence analysis using anti-CI-M6PR and anti-p230 antibodies revealed that most CI-M6PR colocalized with p230 at the TGN and the rest localized to punctate structures, probably endosomes, throughout the cytoplasm. In GSK3β-knockdown cells, several tubules containing CI-M6PR and derived from the TGN were observed relatively frequently (Fig. 2A) and CI-M6PR-positive vesicles accumulated at the cell periphery (Fig. 2A, arrows). The tubular structures in GSK3β-knockdown cells were visualized and analyzed using GFP-tagged CI-M6PR (GFP–CI-M6PR) (Fig. 2B; supplementary material Movies 1 and 2). In control cells, small punctate vesicles that contained GFP–CI-M6PR and that budded from the Golgi were observed frequently. In

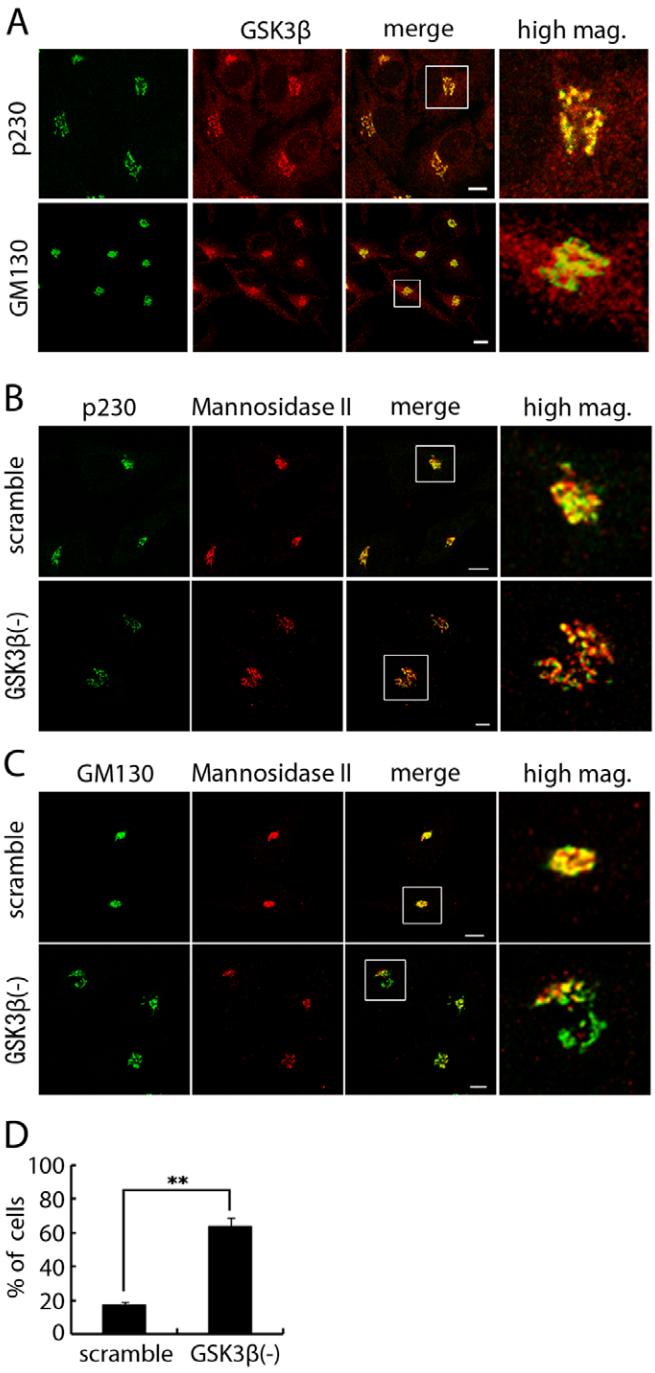

Fig. 1. GSK3β localizes to the TGN and is necessary to maintain Golgi morphology. (**A**) HeLa cells were stained with anti-GSK3β (red), anti-p230 (green), and anti-GM130 (green) antibodies. (**B**) HeLa cells were treated with scramble or GSK3β siRNA for 72 hours, and then stained with anti-p230 (green) and anti-mannosidase II (red) antibodies. (**C**) HeLa cells were treated with scramble or GSK3β siRNA for 72 hours, and then stained with anti-GM130 (green) and anti-mannosidase II (red) antibodies. (**D**) Graph shows average percentage of cells with a fragmented Golgi that dispersed more than 40 μm in the cells. Values are means ± s.d.; n=300, $^{**}P$<0.005 (Student's t-test). Scale bars: 10 μm.

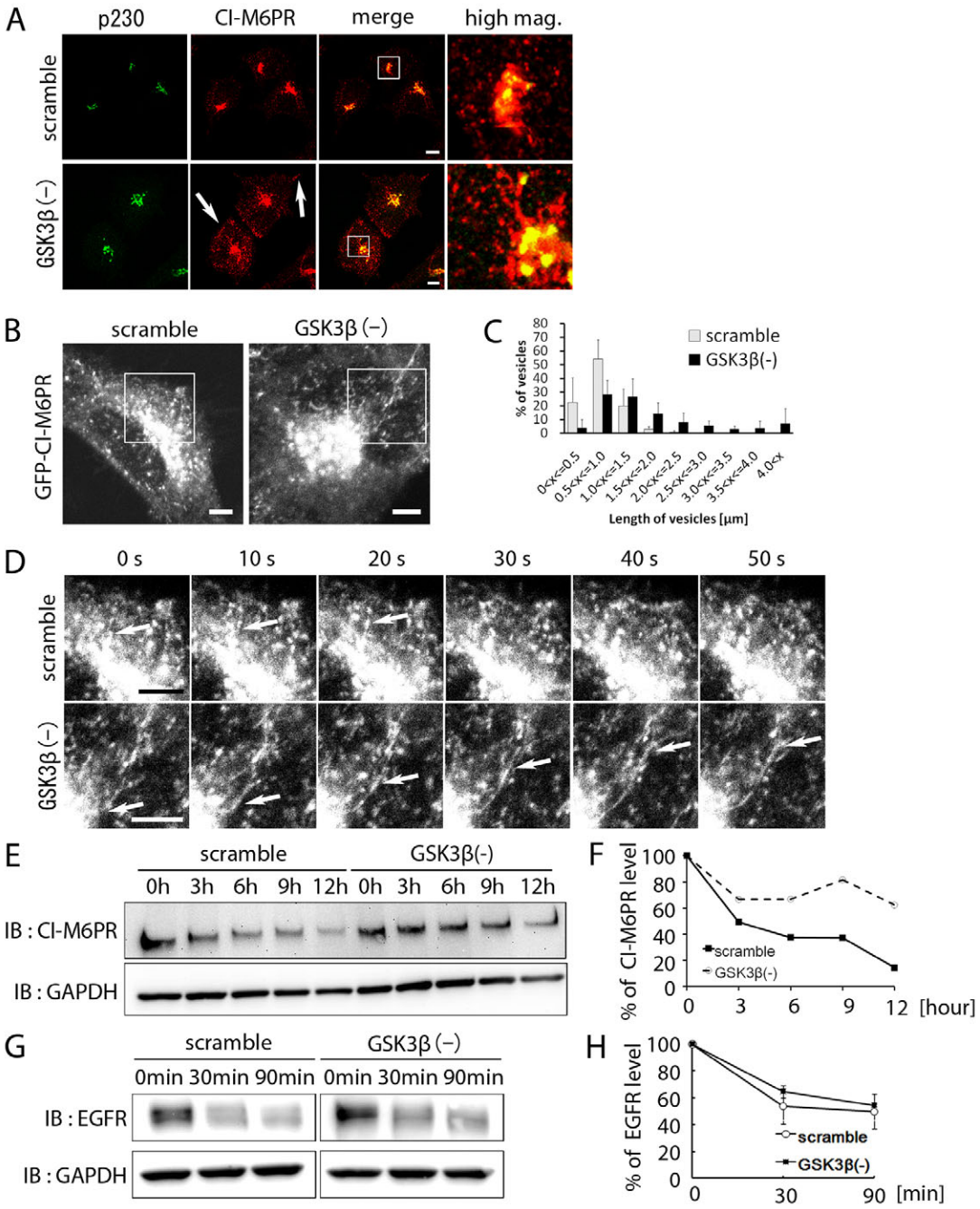

Fig. 2. GSK3β regulates CI-M6PR transport from the Golgi. (**A**) Control (scramble) or GSK3β-knockdown [GSK3β(–)] cells were stained with anti-p230 (green) and anti-CI-M6PR (red) antibodies. Arrows indicate endosomes containing CI-M6PR, which accumulated at the cell periphery. Scale bars: 10 µm. (**B**) Control or GSK3β-knockdown cells were transfected with GFP–CI-M6PR plasmids. After incubation, cells were imaged by time-lapse fluorescence microscopy. Images in this figure were extracted from supplementary material Movie 1 or 2. Scale bars: 5 µm. (**C**) The length of GFP–CI-M6PR carriers (tubules and vesicles) was measured using the data in B. The amount of carriers was set as 100% for each cell. Values are means ± s.d.; n=10. (**D**) Time-lapse images of data shown in B. Arrows indicate vesicles budding from the Golgi. Scale bars: 5 µm. (**E**) Immunoblot analysis of CI-M6PR half-life in control and GSK3β-knockdown cells after treatment with 100 µg/ml cycloheximide. GAPDH was used as a loading control. (**F**) Graphical representation of the data shown in E. The level of CI-M6PR was normalized to the level of GAPDH. (**G**) Control or GSK3β-knockdown cells were washed, treated with 10 ng/ml EGF in serum-free medium, and then incubated at 37°C for various periods of time. After washing to remove excess ligand, the cells were lysed and immunoblotted with anti-EGFR antibody. GAPDH was used as a loading control. (**H**) Graphical representation of the data shown in G. The level of EGFR was normalized to the level of GAPDH.

GSK3β-knockdown cells, membranous structures that contained GFP–CI-M6PR appeared to bud but formed long tubular structures rather than smaller carrier vesicles (Fig. 2C). In control cells, the tubules did not exceed 1.5 µm in length, whereas in the GSK3β-knockdown cells, >40% of the budded structures were longer than 1.5 µm (Fig. 2C,D).

To assess CI-M6PR transport between the TGN and PLC, we examined the level of CI-M6PR in cells treated with scramble or

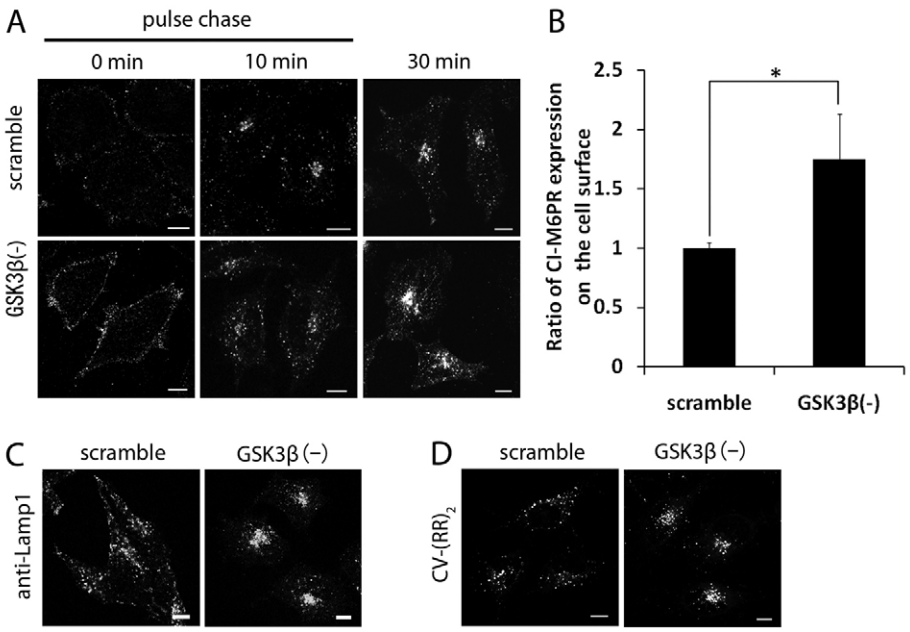

Fig. 3. GSK3β knockdown increases CI-M6PR on the cell surface and inhibits the localization of lysosomal proteins. (**A**) For pulse chase analysis, control (scramble) or GSK3β-knockdown cells were incubated with 10 μg/ml antibody against the luminal domain of CI-M6PR for 0.5 hours on ice. Then, the cells were washed and returned to pre-warmed medium (37°C) for the indicated time. To analyze antibody uptake, control or GSK3β-knockdown cells were incubated with 10 μg/ml antibody against the luminal domain of CI-M6PR for 0.5 hours at 37°C. The cells were fixed and stained with Cy2-conjugated anti-mouse antibody. (**B**) Quantification of CI-M6PR intensity on the cell surface at 0 minutes. The graph shows the amount of CI-M6PR on the cell surface as calculated from the z-stack image shown in A. Values are means ± s.d.; n=40, *P<0.05 (Student's t-test). (**C**) Control or GSK3β-knockdown cells were stained with anti-Lamp1 antibody. (**D**) Control or GSK3β-knockdown cells were treated with CV-$(RR)_2$ probe for 1 hour and then images were acquired by confocal microscopy. Scale bars: 10 μm.

GSK3β siRNA at different times after the inhibition of protein synthesis with cycloheximide (Fig. 2E). After cycloheximide treatment, the level of CI-M6PR decreases faster in cells where retrograde transport is perturbed than in control cells (Arighi et al., 2004; Seaman et al., 2007). We found that, in cells treated with scramble siRNA, CI-M6PR decreased to ~20% of the original level at 12 hours after cycloheximide treatment (Fig. 2F; scramble). In the GSK3β-knockdown cells, the level of CI-M6PR decreased to ~60% of the original level at 12 hours [Fig. 2F; GSK3β(–)]. This suggests that GSK3β knockdown perturbs the anterograde transport of CI-M6PR between the TGN and PLC.

We performed FRAP analysis using GFP–CI-M6PR to examine the effect of GSK3β knockdown on retrograde transport of CI-M6PR from the PLC to the TGN (supplementary material Fig. S3A,B). The kinetics of fluorescence recovery at the Golgi in GSK3β-knockdown cells was indistinguishable from that in control cells. Furthermore, an inhibitor of GSK3, LiCl, had no effect on CI-M6PR retrograde transport (supplementary material Fig. S3C,D), although wortmannin, a phosphoinositide 3-kinase (PI3K) inhibitor that is known to slow retrograde transport of CI-M6PR from endosomes to the Golgi (Kundra and Kornfeld, 1998), did delay fluorescence recovery at the Golgi. These results indicate that GSK3β knockdown did not affect retrograde transport from endosomes or the PM to the Golgi.

To elucidate the effect of GSK3β knockdown on transport from the PLC to lysosomes, we examined EGFR (epidermal growth factor receptor) degradation in lysosomes (Fig. 2G,H). EGF stimulates EGFR internalization via clathrin-dependent endocytosis. EGFR is then transported to lysosomes and degraded. Control or GSK3β-knockdown cells were washed and treated with 10 ng/ml EGF in serum-free medium. After incubation for various periods, the cells were lysed and immunoblotted with anti-EGFR antibody. The kinetics of EGFR degradation was similar in control and GSK3β-knockdown cells. Taken together, these results indicate that GSK3β knockdown has no effect on transport from the PLC to lysosomes, and therefore that it inhibits the anterograde transport of CI-M6PR from the TGN to the PLC rather than affecting its retrograde transport.

GSK3β knockdown causes mis-sorting of CI-M6PR to the cell surface

To determine the destination of mis-sorted CI-M6PR in GSK3β-knockdown cells, we pulse-labeled cell surface CI-M6PR using an antibody against the extracellular portion of CI-M6PR and studied its transport to the cell surface and subsequent endocytosis using immunofluorescence. As a result, we found that cell surface labeling of CI-M6PR was more extensive in GSK3β-knockdown cells than in control cells, and that the amount of antibody uptake, which depends on delivery of CI-M6PR to the cell surface and subsequent endocytosis, during a period of 30 minutes at 37°C was substantially higher in GSK3β-knockdown cells than in control cells (Fig. 3A). The amount of CI-M6PR expression at the cell surface was quantified from indirect immunofluorescence images and was approximately 1.5 times higher in GSK3β-knockdown cells than in control cells (Fig. 3B). This suggested that trafficking of CI-M6PR to the cell surface was facilitated by GSK3β knockdown and that cell surface CI-M6PR was endocytosed rapidly and delivered to the perinuclear region of the GSK3β-knockdown cells, which indicated that normal recycling of CI-M6PR occurred.

We also examined the effect of GSK3β knockdown on the localization of the lysosomal membrane protein Lamp1 using immunofluorescence and that of cathepsin B, a cargo protein for CI-M6PR that is normally sorted to lysosomes by M6PR, using a cell-permeable fluorescent substrate of cathepsin B. We observed that, in control cells, Lamp1 and the fluorescent substrates of cathepsin B localized to punctate structures throughout the cytoplasm (Fig. 3C,D) but, in GSK3β-knockdown cells, they accumulated near the juxtanuclear region, similarly to re-endocytosed CI-M6PR (Fig. 3A). The morphological studies in our previous paper (Adachi et al., 2009) indicated that the organelles that accumulate in the juxtanuclear region in GSK3β-knockdown cells are immunolabeled with antibodies against early and late endosomes, and lysosomes.

Taken together, these results suggest that newly synthesized CI-M6PR and its cargo in GSK3β-knockdown cells are not delivered to the PLC and/or lysosomes but rather are transported to the cell surface (Fig. 3A–D).

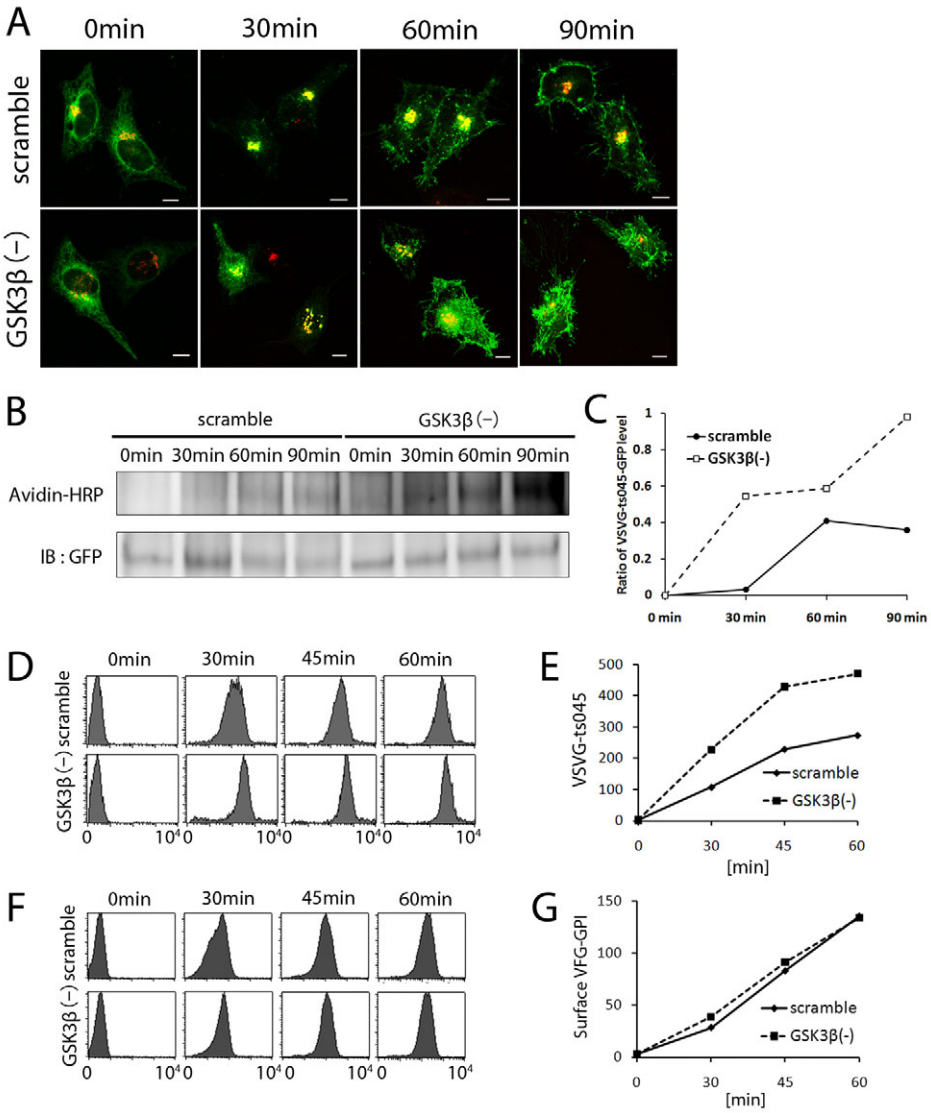

Fig. 4. GSK3β knockdown increases VSVG-ts045 transport from the ER to the PM. (**A**) HeLa cells were treated with scramble or GSK3β siRNA for 48 hours, transfected with VSVG-ts045–GFP plasmid, and then incubated at 40°C for 24 hours. After incubation, the cells were transferred to 32°C to initiate transport from the ER. At the times indicated, cells were fixed and observed by confocal microscopy. (**B**) Biotinylation analysis of the surface expression of VSVG at the indicated times after a temperature shift from 40°C to 32°C. HeLa cell surface proteins were labeled with biotin and then VSVG-ts045–GFP was immunoprecipitated with anti-GFP antibody. VSVG-ts045–GFP on the cell surface was detected by avidin-conjugated HRP and the total VSVG-ts045–GFP was detected with anti-GFP antibody. (**C**) Graph shows the amount of VSVG-ts045–GFP that was biotinylated at the cell surface. (**D**) Flow cytometric analysis of the surface expression of VSVG at the indicated times after a temperature shift from 40°C to 32°C. CHO cells expressing FLAG–VSVG-ts045–EGFP were stained with an anti-FLAG antibody. (**E**) Graph shows the geometrical mean analysis of the data shown in D. (**F**) Flow cytometric analysis of the surface expression of reporter proteins at the indicated times after a temperature shift from 40°C to 32°C. CHO cells expressing VSVG^{ex}–FLAG–EGFP–GPI were stained with an anti-FLAG antibody. (**G**) Graph shows the geometrical mean analysis of the data in F. Scale bars: 10 μm.

GSK3β knockdown facilitates VSVG-ts045 transport from the ER to the PM

To examine the effect of GSK3β knockdown on the transport of newly synthesized glycoproteins, we analyzed the exocytic vesicular transport of VSVG-ts045–GFP (Kano et al., 2009). VSVG-ts045 is a temperature-sensitive type I transmembrane protein from vesicular stomach virus that is used as a tool for studying membrane traffic. By 90 minutes after the chase at 32°C, almost all the VSVG-ts045–GFP had reached the PM in control or GSK3β-knockdown HeLa cells (Fig. 4A). To quantify the extent of transport of VSVG to the PM, we performed two types of experiment: a cell surface labeling assay (avidin–biotin complex assay) and a flow cytometric assay. These assays enabled us to determine the amount of either biotinylated VSVG at the PM or antibody bound to the extracellular part of VSVG, using western blotting or flow cytometry, respectively. As shown in Fig. 4B,C, the amount of cell surface VSVG in GSK3β-knockdown cells increased with increasing time and, after a 90 minute chase, was approximately twice that observed in control cells. We also confirmed the effect of GSK3β knockdown on VSVG transport using Chinese hamster ovary (CHO) cells that stably express FLAG–VSVG-ts045–EGFP from a doxycycline-inducible promoter (Maeda et al., 2008). FLAG–VSVG-ts045–EGFP was transported to the PM slightly faster in GSK3β-knockdown CHO cells than in control cells (Fig. 4D,E). Thus, GSK3β knockdown increased not only the rate of VSVG transport but also the total amount of VSVG at the cell surface in both HeLa and CHO cells. In HeLa cells, we observed that the knockdown had no effect on the endocytosis of VSVG (data not shown). Thus, GSK3β knockdown might cause random or non-regulated vesiculation from the fragmented Golgi, which might in turn facilitate post-Golgi transport. Interestingly, we found that GSK3β knockdown had no effect on the transport of a GPI-anchored protein, FLAG-tagged GPI–VSVG-ts045, to the cell surface in CHO cells (Fig. 4F,G). This indicates that CI-M6PR and VSVG do not use the same post-Golgi trafficking pathways as GPI-anchored proteins.

Next, we investigated the colocalization of VSVG-ts045–GFP and CI-M6PR by immunofluorescence. Sixty minutes after the temperature was shifted to 32°C, the cells were fixed and stained with anti-CI-M6PR antibody. In control cells, vesicles containing both VSVG and CI-M6PR were found on rare occasions (<10% of all vesicles). In GSK3β-knockdown cells, almost all the carriers, tubular structures, and vesicles containing CI-M6PR also contained VSVG (>90%) (Fig. 5A). These results indicate that, in GSK3β-

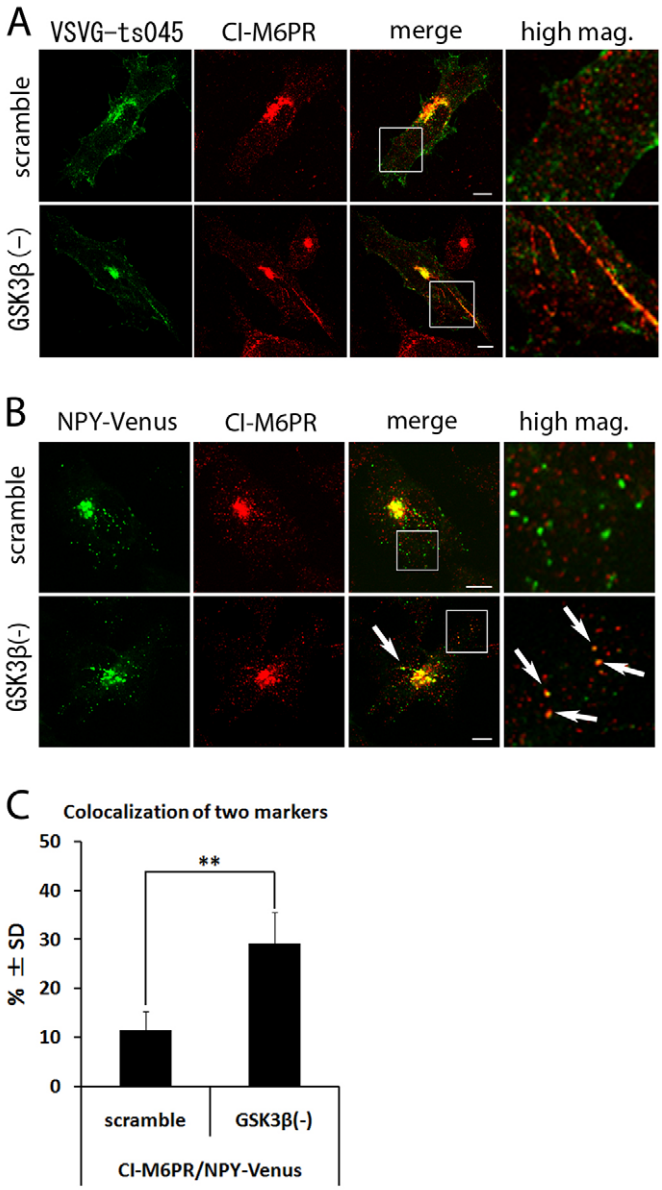

Fig. 5. GSK3β knockdown regulates the transport of exocytic carriers. (**A**) Control (scramble) or GSK3β-knockdown cells were transfected with the VSVG-ts045–GFP plasmid and incubated at 40°C for 24 hours. After incubation, the cells were transferred to 32°C for 1 hour to initiate transport from the ER. Then, the cells were fixed and stained with anti-CI-M6PR (red) antibody. (**B**) Control or GSK3β-knockdown cells were transfected with the NPY–Venus plasmid and incubated for 24 hours. After incubation, the cells were fixed and stained with anti-CI-M6PR (red) antibody. Arrows indicate vesicles or tubules that contained both NPY–Venus and CI-M6PR. (**C**) Quantification of colocalization area in cells prepared as described in B. Graph shows the colocalization area as a proportion of the entire cytoplasmic region, excluding the Golgi. Values are means ± s.d.; n=80, $^{**}P$<0.005 (Student's t-test). Scale bars: 10 μm.

knockdown cells, CI-M6PR might be diverted from the normal pathway of transport to the PLC into the secretory pathway used by VSVG after exit from the TGN. To examine whether the tubules and carriers containing CI-M6PR in GSK3β-knockdown cells were involved in anterograde transport to the PM, we used immunostaining to investigate the colocalization of CI-M6PR with neuropeptide Y fused with Venus (NPY–Venus), which is known to be secreted into the medium by HeLa cells. Then, we estimated the extent of colocalization of the two cargos by calculating the proportion of the total area of carrier that was labeled for both cargos. Morphological and quantitative analysis indicated that the extent of colocalization of the two cargos in the same carrier was approximately 2.5 times higher in GSK3β-knockdown cells than in control cells (Fig. 5B,C). These results indicate that CI-M6PR-positive carriers are involved in anterograde transport.

GSK3β function and association with the TGN is regulated by p230

Due to the extensive colocalization of GSK3β with p230 at the TGN (Fig. 1A), we hypothesized that GSK3β associates with the TGN through p230, and that TGN-associated GSK3β plays a crucial role in regulating the exocytic transport and organization of microtubules around the Golgi complex. To test this, we examined the effect of p230 knockdown on the association of GSK3β with the TGN. We tested three siRNAs that targeted different sequences within the p230 mRNA, and compared their knockdown efficiency in HeLa cells by western blotting with an anti-p230 antibody (Fig. 6A). siRNA #3 decreased the level of p230 to ~10% of that obtained with scramble siRNA. Therefore, we used siRNA #3 to knock down p230 protein. Immunofluorescence with anti-GSK3β and anti-p230 antibodies revealed that, although GSK3β colocalized with p230 extensively in the TGN in control cells, in p230-knockdown cells GSK3β dispersed completely into the cytoplasm (Fig. 6B). To confirm this, we examined the effect of overexpression of p230-truncated mutants on GSK3β association with the TGN. We used two p230 truncation mutants, which corresponded to: (1) 292 amino acids from the N-terminus of p230 tagged with haemagglutinin (HA) (HA–p230-N292), and (2) 312 amino acids from the C-terminus of p230 (containing the GRIP domain) and tagged with HA (HA–p230-C312). At 24 hours after transfection of the plasmids into HeLa cells, the cells were fixed and examined by immunofluorescence. In the HA–p230-C312-transfected cells, GSK3β had disappeared from the TGN and diffused throughout the cytoplasm, although HA–p230-C312 remained associated with the Golgi and tubular structures (Fig. 6C; lower panel). In the N292-transfected cells, HA–p230-N292 was observed throughout the cytoplasm but GSK3β remained associated with the TGN (Fig. 6C; upper panel). Overexpression of HA–p230-C312 induces the diffuse distribution of endogenous GRIP proteins, including p230 (Yoshino et al., 2003). These results demonstrate strongly that the association of GSK3β with the TGN depends on the localization of endogenous p230. To confirm the binding of GSK3β to p230 biochemically, we tried to co-immunoprecipitate the proteins from HeLa cell lysates with anti-GSK3β or anti-p230 antibodies, but our attempts were unsuccessful. We supposed that the detergent used to solubilize p230 might disrupt a weak interaction between the two proteins, or that p230 and GSK3β might interact indirectly via other p230-binding partners (see Discussion).

GSK3β itself undergoes multiple phosphorylation events and the effect on GSK3β activity depends on the amino acid modified. Phosphorylation of Ser9 of GSK3β has an inhibitory effect on GSK3β function. We examined the level of GSK3β phospho-Ser9 in p230-knockdown and control cells using western blotting with an antibody against GSK3β phospho-Ser9 (Fig. 6D). Ser9 was phosphorylated to the same extent in the two cell types, which suggested that p230 knockdown or dissociation of GSK3β from the TGN does not affect GSK3β activity in whole cells. Thus, we

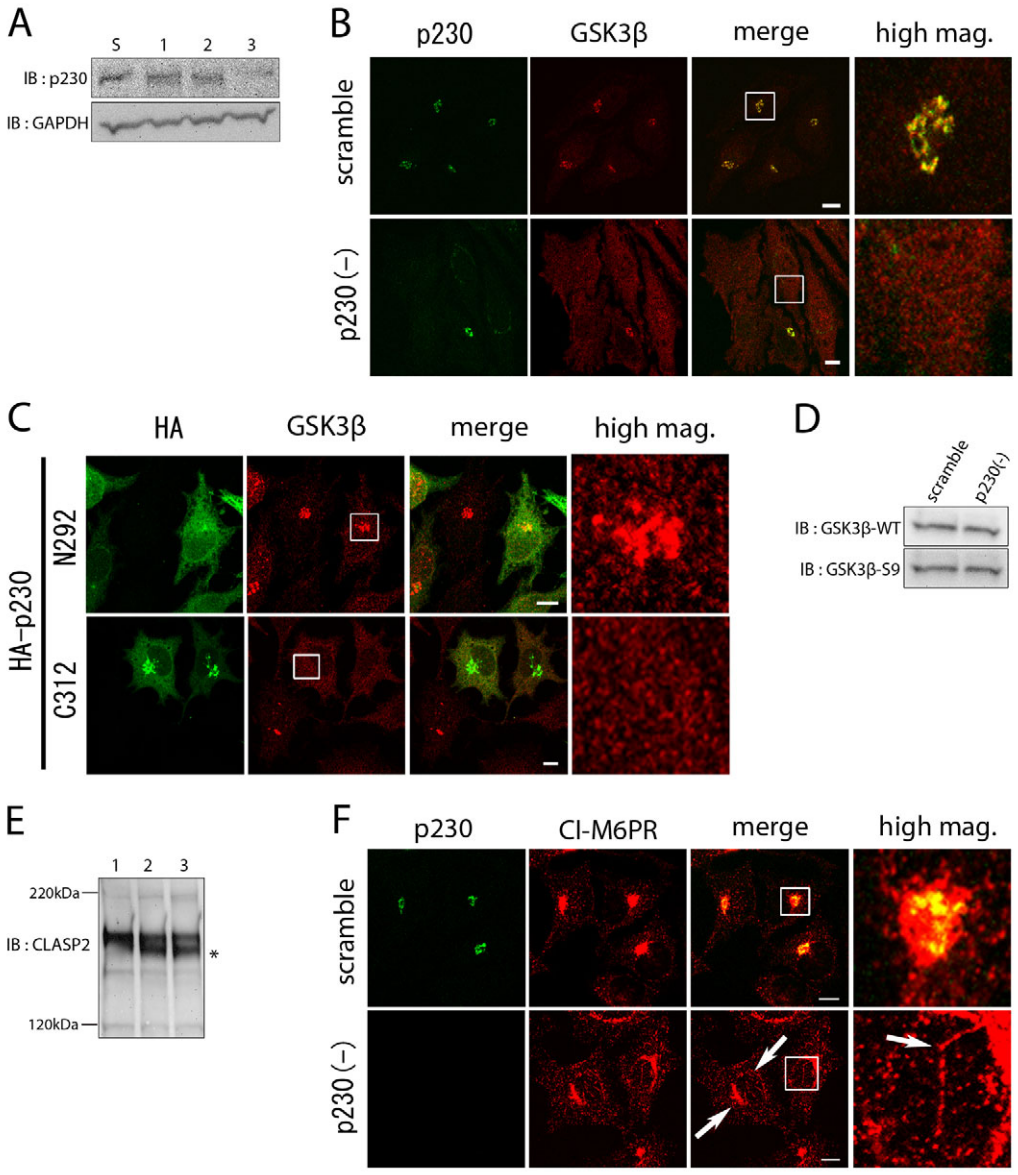

Fig. 6. p230 regulates GSK3β localization to the TGN and CLASP2 phosphorylation. (**A**) Cells transfected with scramble siRNA or one of three different p230 siRNAs were lysed and immunoblotted with anti-p230 and anti-GAPDH antibodies. GAPDH was used as a loading control. Lane S represents lysate from cells transfected with scramble siRNA. Lanes 1, 2 and 3 represent lysates from cells transfected with the three p230 siRNAs, respectively. (**B**) Control or p230-knockdown cells were stained with anti-p230 (green) and anti-GSK3β (red) antibodies. (**C**) HeLa cells were transfected with HA–p230-N292 or HA–p230-C312 plasmids and incubated for 24 hours. After incubation, the cells were stained with anti-HA (green) and anti-GSK3β (red) antibodies. (**D**) Control or p230-knockdown cells were lysed and immunoblotted with anti-GSK3β and anti-phospho-Ser9 GSK3β antibodies. (**E**) Control or p230-knockdown cells were lysed and immunoblotted with anti-CLASP2 antibody. Lane 1, lysate from cells transfected with scramble siRNA; Lane 2, lysate from cells transfected with scramble siRNA and treated with alkaline phosphatase; Lane 3, lysate from cells transfected with p230 siRNA. * denotes the dephosphorylated form of CLASP2. (**F**) Scramble- or p230-knockdown cells were stained with anti-p230 (green) and anti-CI-M6PR (red) antibodies. Arrows indicate tubular structures containing CI-M6PR derived from the TGN. Scale bars: 10 μm.

hypothesized that the target of GSK3β on the Golgi membrane is involved in controlling the Golgi-related events described above. As a consequence, we focused on CLASP2 as a target of GSK3β on the Golgi membranes, and in particular on its phosphorylation status because CLASP2 phosphorylation by GSK3β regulates its function in microtubule dynamics (Kumar et al., 2009). We used western blotting to examine CLASP2 phosphorylation in p230-knockdown cells, in which GSK3β was dissociated from the Golgi (Fig. 6E). We could distinguish the phosphorylation states of CLASP2, using alkaline phosphatase treatment. The upper band corresponds to phosphorylated CLASP2 and the lower band to the dephosphorylated form (Fig. 6E; lane 2 asterisk). In control cells, we detected only the upper band, which indicated that under normal conditions almost all CLASP2 protein was phosphorylated (Fig. 6E; lane 1). By contrast, in the p230-knockdown cells, we detected two bands (Fig. 6E; lane 3), which indicated that a substantial amount of CLASP2 was in the dephosphorylated form in p230-knockdown cells. Finally, we assessed the effect of dissociation of GSK3β from the TGN in p230-knockdown cells on the structure of the exocytic carrier of CI-M6PR, using immunofluorescence with anti-p230 and anti-CI-M6PR antibodies (Fig. 6F). p230 knockdown induced the formation of tubular exocytic carriers containing CI-M6PR, as seen in GSK3β-knockdown cells [Fig. 6F; p230(–) arrows].

TGN-associated GSK3β modulates the interaction of CLASP2 with microtubules

The morphology of the Golgi depends on microtubule integrity. Having found that the Golgi complex was partially fragmented in GSK3β-knockdown cells, we investigated the integrity of microtubules and the centrosome in these cells. We utilized three siRNAs that targeted different sequences within the GSK3β mRNA to rule out off-target effects by the siRNAs. At 48 hours after transfection with scramble siRNA or one of the three siRNAs against GSK3β, cells were transfected with the plasmid encoding GT–GFP. After incubation for 24 hours, the cells were immunostained with antibodies against β-tubulin and γ-tubulin. As shown in Fig. 7A and supplementary material Fig. S4, we confirmed

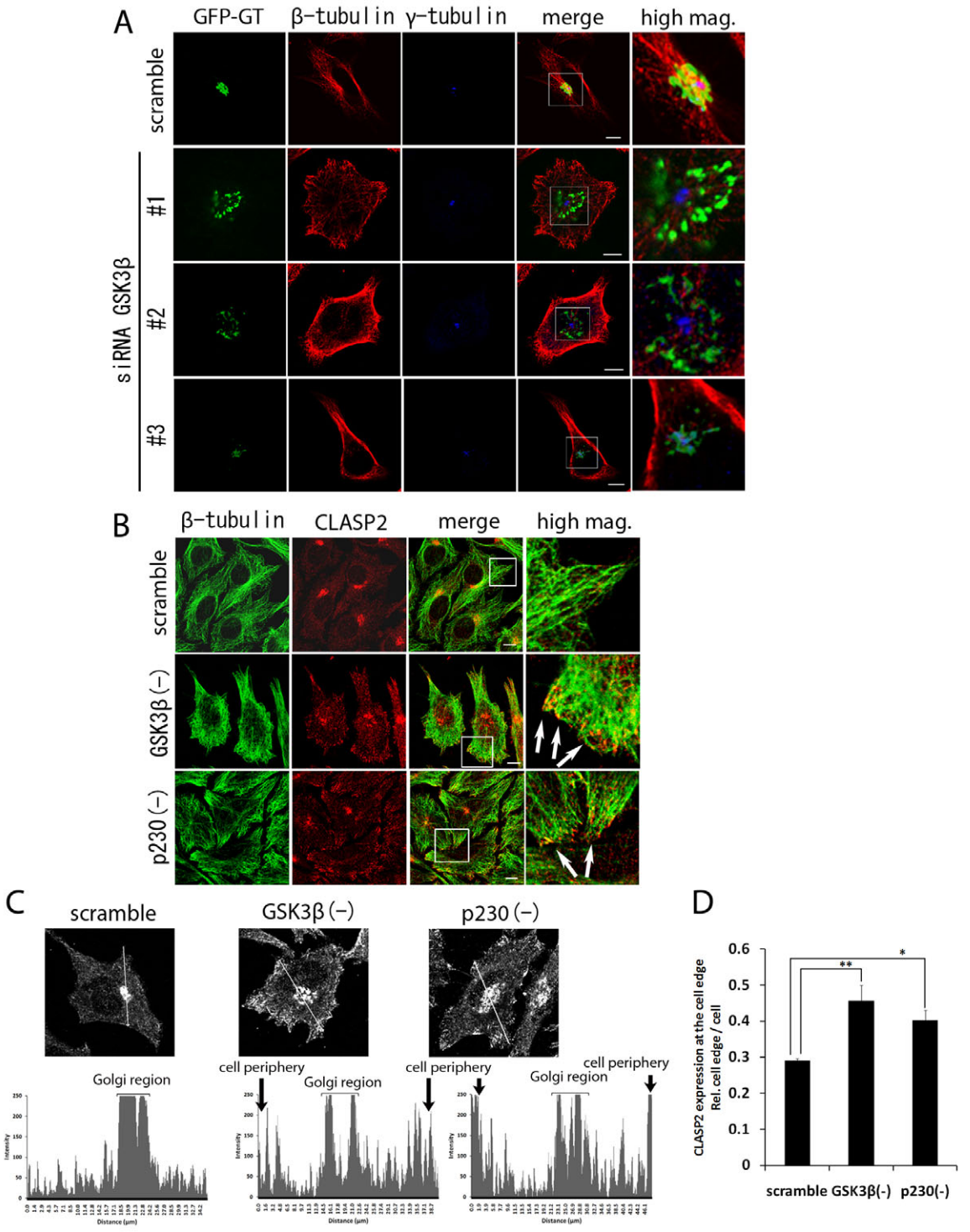

Fig. 7. GSK3β associated with the TGN modulates CLASP2 association with microtubules. (**A**) Control or GSK3β-knockdown cells were transfected with the GT–GFP plasmid and incubated for 24 hours. After incubation, the cells were stained with anti-β-tubulin (red) and anti-γ-tubulin (blue) antibodies. (**B**) Control or GSK3β- or p230-knockdown cells were stained with anti-β-tubulin (green) and anti-CLASP2 (red) antibodies. Arrows indicate accumulation of CLASP2 at the cell periphery. (**C**) Quantification of CLASP2 intensity in the cell. The graph shows the quantification of CLASP2 intensity along the arrow in the image above. (**D**) Quantification of fluorescence intensity of CLASP2 at the cell edge. The fluorescence intensity at the cell edge was measured within the area 5 μm from the cell surface. The graph shows the amount of CLASP2 at the cell edge as a proportion of total CLASP2 in the cell. Values are means ± s.d.; n=60, $^{**}P$<0.005, $^{*}P$<0.05 (Student's t-test). Scale bars: 10 μm.

that all three siRNA probes induced the same phenotype with respect to the integrity of microtubules: the normal radial arrays of microtubules (red fluorescence) associated with a γ-tubulin-positive centrosome (blue fluorescence) and with the Golgi membranes (green fluorescence) were almost entirely absent in GSK3β-knockdown HeLa cells. All three GSK3β siRNAs reduced the

number of microtubules that were associated with the centrosome or the Golgi membranes. These results indicate that GSK3β is involved in Golgi morphology through the organization of microtubule integrity around the Golgi complex and centrosome.

Interestingly, dramatic re-localization of CLASP2 was also observed in GSK3β-knockdown cells. In these cells, CLASP2 accumulated extensively at microtubule plus ends at the cell periphery [Fig. 7B; GSK3β(–) arrows]. Similar accumulation of CLASP2 at microtubule plus ends was seen in p230-knockdown cells [Fig. 7B; p230(–) arrows]. To confirm this more quantitatively, we first obtained representative dual immunofluorescence images of microtubules (green) and CLASP2 (red) for individual cells, and then compared the total intensity of red fluorescence in the peripheral region (5 μm in width from the cell edge) of GSK3β-knockdown cells and control cells (Fig. 7C,D). These results showed that the proportion of CLASP2 at the cell periphery was higher in GSK3β-knockdown cells than in control cells.

These results indicate that Golgi-associated GSK3β might modulate the localization or dynamics of the interaction of CLASP2 with microtubules, and thus regulate the morphology of the Golgi and mis-sorting of CI-M6PR at the TGN.

Discussion

Our findings in this study demonstrate that a portion of GSK3β is localized to the TGN through the Golgi peripheral protein p230 and acts as a guide for post-Golgi membrane trafficking, especially CI-M6PR sorting at the TGN, by regulating the affinity of CLASP2 for microtubules.

GSK3β localizes to the TGN

We found that a substantial portion of GSK3β localized to the TGN (Fig. 1A) and this was independent of the cell cycle or treatment with LiCl (data not shown). Several lines of evidence from our study suggest that p230, a peripheral membrane protein of the TGN, is essential for GSK3β localization to the TGN. p230 knockdown or overexpression of the C-terminal portion of p230 (HA–p230-C312) induced the dissociation of GSK3β from the TGN (Fig. 6B,C), although p230 remained associated with the TGN in GSK3β-knockdown cells. Yoshino and co-workers have shown that overexpression of HA–p230-C312 induces the diffuse distribution of endogenous GRIP proteins, including p230, but overexpression of HA–p230-N292 does not induce (Yoshino et al., 2003). These results might indicate that the middle portion of p230 is involved in the interaction with GSK3β and that disruption of the interaction by overexpression of HA–p230-C312 induces the dissociation of GSK3β from the TGN. Although we could not detect a direct interaction between GSK3β and p230, these results indicate that p230 regulates GSK3β localization to the TGN, which enables GSK3β to phosphorylate a variety of TGN-localized proteins and regulate their functions. We suppose that the interaction between p230 and GSK3β is indirect and that additional TGN-associating protein(s) might be involved in the interaction. One of the most plausible candidates is microtubule–actin crosslinking factor 1 (MACF1) because MACF1 has been shown to interact with GSK3β and p230, localizes to the TGN, and is known to regulate the localization of CLASP2 to the plasma membrane (Chen et al., 2006; Kakinuma et al., 2004; Lin et al., 2005; Drabeck et al., 2006). On the other hand, CLASP2 has been shown to interact with another TGN golgin, GCC185 (Efimov et al., 2007). It is possible that the p230–MACF1–GSK3β complex interacts with the GCC185–CLASP2 complex at the TGN and that this interaction plays a crucial role in CLASP2-mediated microtubule dynamics, both around the TGN and at the cell periphery. The perturbation of this interaction might result in defects in post-Golgi transport such as the mis-sorting of CI-M6PR at the TGN. Lieu and co-workers demonstrated that p230 knockdown inhibits tumor necrosis factor (TNF) transport to the PM in macrophages (Lieu et al., 2008), which suggests that the involvement of p230 in TNF secretion might be regulated by GSK3β at the TGN.

GSK3β plays a crucial role in CI-M6PR transport from the TGN to the PLC

To define the role of Golgi-associated GSK3β in post-Golgi membrane trafficking, we analyzed the transport of CI-M6PR, which cycles mainly from the TGN to the PLC. Immunofluorescence revealed that GSK3β knockdown induced the frequent formation of tubular carriers, which contained CI-M6PR, from the TGN (Fig. 2). We observed that trafficking of CI-M6PR to the cell surface was facilitated in GSK3β-knockdown cells, as compared with control cells, which resulted in the increased transport of CI-M6PR to the PM. In addition, our data showed that cell surface CI-M6PR was endocytosed rapidly and delivered to the perinuclear region of the cells, which suggested that normal recycling of CI-M6PR occurred in GSK3β-knockdown cells. In addition, we confirmed that CI-M6PR colocalized in Golgi-derived carriers (tubules and vesicles) with the exocytic transport cargos VSVG and neuropeptide Y (NPY), which we found to be involved in anterograde transport (Fig. 5). These results suggested that CI-M6PR in GSK3β-knockdown cells shows a preference for the anterograde transport pathway rather than the pathway to the PLC. Indeed, a cycloheximide chase experiment showed that lysosomal degradation of CI-M6PR in GSK3β-knockdown cells was slower than that in control cells (Fig. 2E,F). FRAP analysis using GFP–CI-M6PR revealed that GSK3β knockdown did not affect the retrograde transport of CI-M6PR from the PLC to the TGN (see supplementary material Fig. S3). Furthermore, we found that the knockdown had no effect on the transport of endocytosed EGFR from the PLC to lysosomes. Therefore, GSK3β knockdown might disturb the sorting of CI-M6PR at the TGN to the PLC, without affecting retrograde transport. We suppose that PM-targeted carriers (vesicles) containing mis-sorted CI-M6PR might contain so many cargos that vesicles are transformed into long tubules to enhance the transport.

GSK3β is involved in the microtubule dynamics or local microtubule stability through the phosphorylation of CLASP2

GSK3β regulates microtubule dynamics by phosphorylating a variety of substrates, including microtubule-associated proteins and plus-end tracking proteins. We found that GSK3β knockdown reduced the intensity of microtubules around the MTOC (Fig. 7A; supplementary material Fig. S4), which was consistent with the result reported by Fumoto and co-workers (Fumoto et al., 2006). In addition, we observed that the number of microtubules associated with the Golgi was also decreased in GSK3β-knockdown cells (Fig. 7A; supplementary material Fig. S4). Given that the morphology of the Golgi depends largely on microtubule integrity, these changes in the microtubule array could explain the partial disruption of the Golgi complex that is observed in GSK3β-knockdown cells.

One of the proteins that are phosphorylated by GSK3β is CLASP2. CLASP2 is a microtubule-associated protein and its

phosphorylation by GSK3β influences its association with microtubules and local microtubule stability (Akhmanova et al., 2001; Wittmann and Waterman-Storer, 2005; Adachi et al., 2009). Furthermore, other groups have reported that binding to microtubules and the asymmetric distribution of CLASP2 at the cell leading edge are regulated by GSK3β (Kumar et al., 2009; Akmanova et al., 2001). In fact, we observed that CLASP2 accumulated extensively at the microtubule plus ends at the cell periphery in GSK3β-knockdown cells (Fig. 7C). A similar accumulation of CLASP2 at microtubule plus ends was seen in p230-knockdown cells (Fig. 7C). These results suggest the possibility that Golgi-associated GSK3β regulates the recruitment of CLASP2 to microtubules through phosphorylation. However, it is also possible that cytoplasmic GSK3β, not Golgi-associated GSK3β, regulates CLASP2. In fact, it has been reported that cytoplasmic CLASP2 that has been dissociated from the TGN by brefeldin A treatment retains its ability to promote Golgi-derived microtubule formation (Efimov et al., 2007). More studies are needed to distinguish the effects of Golgi-associated and cytoplasmic GSK3β on the activity of CLASP2.

Recently, several groups have shown the role of CLASPs in the formation of Golgi-derived microtubules. Efimov and co-workers demonstrated that CLASPs regulate asymmetric microtubule nucleation at the Golgi (Efimov et al., 2007). In addition, Miller and co-workers have reported that CLASP-dependent Golgi-derived microtubules are required for Golgi organization and polarized membrane trafficking (Miller et al., 2009). Furthermore, Wang and colleagues have reported that unstacking of the Golgi facilitates the post-Golgi transport of CD8 to the cell surface (Wang et al., 2008). Our results might support a possible mechanistic model in which Golgi-derived CLASP-dependent microtubules, which are regulated by GSK3β phosphorylation, control the organization of the Golgi and are involved in the sorting of cargo at the TGN. However, we could not determine whether the disruption of Golgi-associated microtubules caused the mis-sorting at the Golgi or whether these phenomena were unrelated. To address this issue, it will be necessary to establish an in vivo or in vitro assay that enables the sorting process to be measured sensitively and quantitatively, and to examine more extensively how Golgi-associated GSK3β and CLASP2 are involved in the process.

In summary, our results showed that GSK3β localized to the Golgi in a p230-dependent manner, and indicate a new role of Golgi-associated GSK3β in post-Golgi trafficking, especially in the sorting of cargo at the TGN.

Materials and Methods

Cell culture

HeLa cells were cultured in DMEM (Nissui) supplemented with 10% fetal bovine serum (FBS; GIBCO) and penicillin/streptomycin (GIBCO).

Antibodies

The following primary antibodies were used: rabbit antibodies against GSK3β (Cell Signaling), phospho-Ser9-GSK3β (Cell Signaling), EGFR (sc-03; Santa Cruz Biotechnology), mannosidase II (Chemicon), actin (A-5060; Sigma Aldrich), CI-M6PR (IBL), CLASP2 (a gift from Irina Kaverina, Vanderbilt University Medical Center, Nashville, TN), γ-tubulin (T5192; Sigma Aldrich), GFP (MBL), mouse monoclonal antibodies against CD222 (Serotec), GAPDH (MAB374; Chemicon), β-tubulin (T4026; Sigma Aldrich), Lamp1 (H4B3; Developmental Studies Hybridoma Bank, University of Iowa, Iowa City, IA), p230 (BD Biosciences), γ-tubulin (T3559; Sigma Aldrich), and GM130 (BD Biosciences); and a rat monoclonal anti-HA antibody (3F10; Roche). The following secondary antibodies were used for western blotting: horse radish peroxidase (HRP)-conjugated anti-mouse (Upstate Biotechnology) and anti-rabbit antibodies (Chemicon). The following secondary antibodies were used for immunofluorescence: Cy2-conjugated anti-mouse or anti-rabbit antibodies (Chemicon), Cy3-conjugated anti-mouse or anti-rabbit antibodies (Chemicon), and Cy5-conjugated anti-rabbit antibodies (Chemicon).

Chemicals and plasmids

Nocodazole and cycloheximide were purchased from Sigma Aldrich. Wortmannin was purchased from Calbiochem. These inhibitors were diluted at appropriate concentrations in DMSO and stored at –20°C. Propidium iodide (PI) was purchased from Invitrogen. The VSVG-ts045–GFP construct was a gift from Jennifer Lippincott-Schwartz (National Institutes of Health, Bethesda, MD) and the GFP–CI-M6PR construct was a gift from Satoshi Waguri (Fukushima Medical University, Fukushima, Japan). The GT–GFP construct was performed as described previously (Kano et al., 2004). The HA–p230-N292 and HA–p230-C312 constructs were a gift from Michael S. Marks (University of Pennsylvania, Philadelphia, PA).

Plasmids and siRNA transfection

For plasmid transfection, cells were transfected using Lipofectamine LTX reagent (Invitrogen) according to the manufacturer's instructions. Pre-designed siRNA oligonucleotides that targeted human GSK3β and p230 were purchased from Applied BioSystems. For gene silencing of HeLa cells by siRNA transfection, cells were transfected with 50 nM siRNA using Lipofectamine 2000 (Invitrogen) according to the manufacturer's instructions.

Immunofluorescence microscopy

Indirect immunofluorescence microscopy was performed according to the methods described previously (Kano et al., 2004). To quantify CI-M6PR colocalization with NPY–Venus, we measured the fluorescence intensity of the cytosolic region, excluding the Golgi region, in control and GSK3β-knockdown cells expressing NPY–Venus. We then quantified the area of colocalization using the LSM 510 software package. To quantify the fluorescence intensity of CLASP2 at the cell edge, we measured the fluorescence intensity of the area within a distance of 5 μm from the cell edge and the fluorescence within the whole cell using the LSM 510 software package. We calculated the fluorescence intensity at the cell edge as a proportion of the fluorescence throughout the whole cell.

Cycloheximide chase assay

Cells were incubated in DMEM containing 10% FBS and 100 μg/ml cycloheximide. At the relevant time points, the cells were lysed and analyzed by SDS-PAGE and immunoblotting.

Measurements of cathepsin B activity in vivo

Scramble or specific siRNA-treated cells were grown on 35-mm glass-based dishes. Cathepsin B activity in the cells was quantified using a CV-cathepsin B Detection Kit (BIOMOL) according to the manufacturer's instructions. Images were acquired with an LSM510 confocal microscope (Carl Zeiss). CV-$(RR)_2$ probes were excited at a wavelength of 550 nm and imaged through a >610 nm long-pass emission filter.

VSVG-ts045–GFP transport assay

Cells were transfected with the VSVG-ts045–GFP plasmid and then incubated for 24 hours at 40°C. They were then transferred to 32°C to initiate transport from the ER and incubated. At the relevant time points, the cells were fixed and immunostained with anti-GM130 antibody. For the biotinylation assay, the cells were washed three times with ice-cold PBS (pH 8.0), agitated gently at 4°C for 30 minutes in PBS containing 1 mg/mL sulfo-NHS–biotin, and then washed three times in PBS with 100 mM glycine. The cells were lysed on ice in RIPA buffer containing Complete Protease Inhibitor Cocktail (Roche). Cell lysates were incubated for 4 hours at 4°C with anti-GFP antibody and protein G–Sepharose beads (GE Healthcare). The precipitates were then washed three times with lysis buffer. The proteins were separated by SDS-PAGE and analyzed by immunoblotting with a Vectastain Elite ABC kit (Vector Labs). The flow cytometric transport assay was performed according to methods previously described (Takida et al., 2008; Maeda et al., 2008).

EGFR degradation assay

Cells were loaded with 10 ng/ml EGF (PEPRO Tech), and incubated. At the relevant time points, the cells were washed, lysed, and analyzed by SDS-PAGE and immunoblotting.

Time-lapse fluorescence microscopy

HeLa cells grown to 40–50% confluency on 35-mm glass-bottomed culture dishes (Asahi Techno Glass) were transfected with a plasmid encoding GFP–CI-M6PR. At 24 hours after transfection, time-lapse imaging was performed using a 64× oil immersion objective on an LSM 510 confocal microscope (Carl Zeiss). Time-lapse images were acquired every 10 seconds by scanning the specimen with a low power laser (5%) using a pinhole size of 3 μm. The image sequences were processed and the length of CI-M6PR-containing vesicles was quantified using the LSM 510 software package. For time-lapse imaging, we performed three independent transport assays and measured the CI-M6PR signal of at least ten cells for each condition. The means and s.d. were plotted.

We thank K. Osaka, N. Okamoto, and M. Ueki for experimental assistance. This work was supported by grants from the Ministry of Education, Culture, Sports, Science and Technology of Japan (21113504 to M.M.), National Institute of Biomedical Innovation (to M.M.), and PRESTO from the Japan Science and Technology Agency (to F.K.).

Supplementary material available online at
http://jcs.biologists.org/cgi/content/full/123/19/3215/DC1

References

Adachi, A., Kano, F., Saido, T. C. and Murata, M. (2009). Visual screening and analysis for kinase-regulated membrane trafficking pathways that are involved in extensive beta-amyloid secretion. *Genes Cells* **3**, 355-369.

Akhmanova, A., Hoogenraad, C. C., Drabek, K., Stepanova, T., Dortland, B., Verkerk, T., Vermeulen, W., Burgering, B. M., De Zeeuw, C. T., Grosveld, F. et al. (2001). Clasps are CLIP-115 and -170 associating proteins involved in the regional regulation of microtubule dynamics in motile fibroblasts. *Cell* **104**, 923-935.

Arighi, C. N., Hartnell, L. M., Aguilar, R. C., Haft, C. R. and Bonifacino, J. S. (2004). Role of the mammalian retromer in sorting of the cation-independent mannose 6-phosphate receptor. *J. Cell Biol.* **165**, 123-133.

Bossard, C., Bresson, D., Polishchuk, R. S. and Malhotra, V. (2007). Dimeric PKD regulates membrane fission to form transport carriers at the TGN. *J. Cell Biol.* **179**, 1123-1131.

Chen, H. J., Lin, C. M., Lin, C. S., Perez-Olle, R., Leung, C. L. and Liem, R. K. (2006). The role of microtubule actin cross-linking factor 1 (MACF1) in the Wnt signaling pathway. *Genes Dev.* **20**, 1933-1945.

Drabek, K., van Ham, M., Stepanova, T., Draegestein, K., van Horssen, R., Sayas, C. L., Akhmanova Ten Hagen, A. T., Smits, R., Fodde, R., Grosveld, F. et al. (2006). Role of CLASP2 in microtubule stabilization and the regulation of persistent motility. *Curr. Biol.* **16**, 2259-2264.

Efimov, A., Kharitonov, A., Efimova, N., Loncarek, J., Miller, P. M., Andreyeva, N., Gleeson, P., Galjart, N., Maia, A. R., McLeod, I. X. et al. (2007). Asymmetric CLASP-dependent nucleation of noncentrosomal microtubules at the trans-Golgi network. *Dev. Cell.* **12**, 917-930.

Fischer, H. D., Gonzalez-Noriega, A. and Sly, W. S. (1980). β-glucuronidase binding to human fibroblast membrane receptors. *J. Biol. Chem.* **255**, 5069-5074.

Fumoto, K., Hoogenraad, C. C. and Kikuchi, A. (2006). GSK-3beta-regulated interaction of BICD with dynein is involved in microtubule anchorage at centrosome. *EMBO J.* **25**, 5670-5682.

Garczarczyk, D., Toton, E., Biedermann, V., Rosivatz, E., Rechfeld, F., Rybczynska, M. and Hofmann, J. (2009). Signal transduction of constitutively active protein kinase C epsilon. *Cell. Signal.* **5**, 745-752.

Gärtner, A., Huang, X. and Hall, A. (2006). Neuronal polarity is regulated by glycogen synthase kinase-3 (GSK-3beta) independently of Akt/PKB serine phosphorylation. *J. Cell. Sci.* **119**, 3927-3934.

Grimes, C. A. and Jope, R. S. (2001). The multifaceted roles of glycogen synthase kinase 3beta in cellular signaling. *Progr. Neurobiol.* **65**, 391-426.

Kakinuma, T., Ichikawa, H., Tsukada, Y., Nakamura, T. and Toh, B. H. (2004). Interaction between p230 and MACF1 is associated with transport of a glycosyl phosphatidyl inositol-anchored protein from the Golgi to the cell periphery. *Exp. Cell Res.* **298**, 388-398.

Kano, F., Tanaka, A. R., Yamauchi, S., Kondo, H. and Murata, M. (2004). Cdc2 kinase-dependent disassembly of endoplasmic reticulum (ER) exit sites inhibits ER-to-Golgi vesicular transport during mitosis. *Mol. Biol. Cell* **15**, 4289-4298.

Kano, F., Yamauchi, S., Yoshida, Y., Watanabe-Takahashi, M., Nishikawa, K., Nakamura, N. and Murata, M. (2009). Yip1A regulates the COPI-independent retrograde transport from the Golgi complex to the ER. *J. Cell Sci.* **122**, 2218-2227.

Kumar, P., Lyle, K. S., Gierke, S., Matov, A., Danuser, G. and Wittmann, T. (2009). GSK3beta phosphorylation modulates CLASP-microtubule association and lamella microtubule attachment. *J. Cell Biol.* **184**, 895-908.

Kundra, R. and Kornfeld, S. (1998). Wortmannin retards the movement of the mannose 6-phosphate/insulin-like growth factor II receptor and its ligand out of endosomes. *J. Biol. Chem.* **273**, 3748-3853.

Lansbergen, G., Grigoriev, I., Mimori-Kiyosue, Y., Ohtsuka, T., Higa, S., Kitajima, I., Demmers, J., Galjart, N., Houtsmuller, A. B., Grosveld, F. et al. (2006). CLASPs attach microtubule plus ends to the cell cortex through a complex with LL5β. *Dev. Cell.* **11**, 21-32.

Lieu, Z. Z., Lock, J. G., Hammond, L. A., La Gruta, N. L., Stow, J. L. and Gleeson, P. A. (2008). A trans-Golgi network golgin is required for the regulated secretion of TNF in activated macrophages in vivo. *Proc. Natl. Acad. Sci. USA* **105**, 3351-3356.

Lin, C. M., Chen, H. J., Leung, C. L., Parry, D. A. and Liem, R. K. (2005). Microtubule actin crosslinking factor 1b: a novel plakin that localizes to the Golgi complex. *J. Cell. Sci.* **118**, 3727-3738.

Maeda, Y., Ide, T., Koike, M., Uchiyama, Y. and Kinoshita, T. (2008). GPHR is a novel anion channel critical for acidification and functions of the Golgi apparatus. *Nat. Cell Biol.* **10**, 1135-1145.

Miller, P. M., Folkmann, A. W., Maia, A. R., Efimova, N., Efimov, A. and Kaverina, I. (2009). Golgi-derived CLASP-dependent microtubules control Golgi organization and polarized trafficking in motile cells. *Nat. Cell Biol.* **9**, 1069-1080.

Salvarezza, S. B., Deborde, S., Schreiner, R., Campagne, F., Kessels, M. M., Qualmann, B., Caceres, A., Kreitzer, G. and Rodriguez-Boulan, E. (2009). LIM kinase **1** and cofilin regulate actin filament population required for dynamin-dependent apical carrier fission from the trans-Golgi network. *Mol. Biol. Cell* **1**, 438-451.

Scheel, J., Matteoni, R., Ludwig, T., Hoflack, B. and Kreis, T. E. (1990). Microtubule depolymerization inhibits transport of cathepsin D from the Golgi apparatus to lysosomes. *J. Cell. Sci.* **96**, 711-720.

Seaman, M. N. (2007). Identification of a novel conserved sorting motif required for retromer-mediated endosome-to-TGN retrieval. *J. Cell. Sci.* **120**, 2378-2389.

Takida, S., Maeda, Y. and Kinoshita, T. (2008). Mammalian GPI-anchored proteins require p24 proteins for their efficient transport from the ER to the plasma membrane. *Biochem. J.* **409**, 555-562.

Waguri, S., Dewitte, F., Le Borgne, R., Rouillé, Y., Uchiyama, Y., Dubremetz, J. F. and Hoflack, B. (2003). Visualization of TGN to endosome trafficking through fluorescently labeled MPR and AP-1 in living cells. *Mol. Biol. Cell* **14**, 142-155.

Wang, Y., Wei, J. H., Bisel, B., Tang, D. and Seemann, J. (2008). Golgi cisternal unstacking stimulates COPI vesicle budding and protein transport. *PLoS ONE* **3,** e1647.

Wittmann, T. and Waterman-Storer, C. M. (2005). Spatial regulation of CLASP affinity for microtubules by Rac1 and GSK3beta in migrating epithelial cells. *J. Cell Biol.* **169**, 929-939.

Yoshino, A., Bieler, B. M., Harper, D. C., Cowan, D. A., Sutterwala, S., Gay, D. M., Cole, N. B., McCaffery, J. M. and Marks, M. S. (2003). A role for GRIP domain proteins and/or their ligands in structure and function of the trans Golgi network. *J. Cell Sci.* **116**, 4441-4454.